
Mechanical properties of NiTi matrix composites reinforced with carbon nanotubes

Xuan Gu, Xiaoyu Sun ^{a,*}, Zheng He ^{b,*}, Lidan Xu, Ju Liu, Binsheng Wang ^{c,*}

College of Aerospace and Civil Engineering, Harbin Engineering University, Harbin
150001 China

^asunxiaoyu520634@163.com, ^bhezhen@hrbeu.edu.cn, ^cwangbinsheng@hrbeu.edu.cn

Abstract

To enhance the mechanical strength of NiTi, 0.5 vol% CNT/NiTi composite was fabricated by high-energy ball milling followed by spark plasma sintering. NiTi and 1 vol% TiC/NiTi composites were also fabricated using the same process for comparison. Unreacted CNTs were observed in the CNT/NiTi composites, although some CNTs had reacted with Ti to form a TiC phase. Thermal hysteresis increased with the addition of CNTs due to increased frictional resistance to interfacial motion between CNT and NiTi matrix, and relaxation of the elastic strain energy in the NiTi matrix. The addition of CNTs, however, had little influence on the shape memory effect of NiTi. The elastic modulus, yield strength and ultimate tensile strength of the 0.5 vol% CNT/NiTi composite were greater than that of the NiTi. This improvement was attributed to the effective load transfer to the unreacted CNTs.

Keywords

Metal matrix composites; Sintering; Shape memory; Mechanical properties.

1. Introduction

Shape memory alloys (SMAs) have unique properties, including shape memory and superelasticity due to a phase transformation between the martensite and austenite phases. When compared with Cu- and Fe-based SMAs, NiTi SMAs are highly corrosion resistant and boast a superior shape memory effect. NiTi SMAs that are subjected to strain of up to 8% can be returned back to its original shape by heating^[1]. Consequently, NiTi SMAs can be used in tribological, pipe coupling, and seismic applications. However, the low mechanical strength and elastic modulus of NiTi SMAs are major obstacles to broadening their applications.

In this paper, we describe the preparation of CNT-reinforced NiTi matrix composites through a powder metallurgical process using CNTs, and Ni and Ti elemental powders. Spark plasma sintering (SPS), which requires a very short time to sinter metal and ceramic powders, was applied to consolidate the CNT/NiTi composite powder. The effect of the CNTs on the mechanical properties of the composites was investigated. TiC/NiTi composites were also fabricated using the same process in order to directly compare their mechanical properties with those of the CNT/NiTi composites.

2. Experimental

Nickel powder (Kojundo, ca. 2–3- μm particle diameter), titanium powder (Kojundo, particle diameter less than 38 μm), CNT powder (Hanwha Nanotech, diameter 10–20 nm and length 10–20 μm), and titanium carbide powder (H.C. Starck, particle diameter less than 5 μm) were used as the starting materials. The microstructures of the raw materials are shown in Fig. 1.

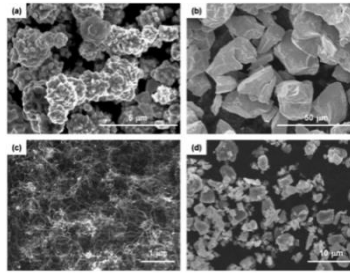


Fig. 1. SEM images of raw materials (a) Ni powder, (b) Ti powder, (c) CNT powder and (d) TiC powder.

3. Results and discussion

Fig. 2 shows the microstructure of the as-milled NiTi powder, the 0.5 vol% CNT/NiTi and 1.0 vol% TiC/NiTi composite powders. The Ni and Ti powders were repeatedly bonded and broken during the high-energy ball-milling process. The Ni and Ti powders were mechanically alloyed due to the high impact energy of the balls, resulting in large particles with diameters greater than 50 μm , as shown in the inset images of Fig. 2. As indicated in Fig. 2(b), the CNTs were homogeneously dispersed in the 0.5 vol% CNT/NiTi composite powder. CNTs that were agglomerated by van der Waals forces were disentangled by the high impact energy of the balls during the milling process. Fig. 2(c) shows the morphology of the 1.0 vol% TiC/NiTi composite powder. It was assumed that the TiC particles were uniformly dispersed in the 1.0 vol% TiC/NiTi composite, although discrete TiC particles were not observed since they were embedded in the mechanically alloyed Ni and Ti powders.

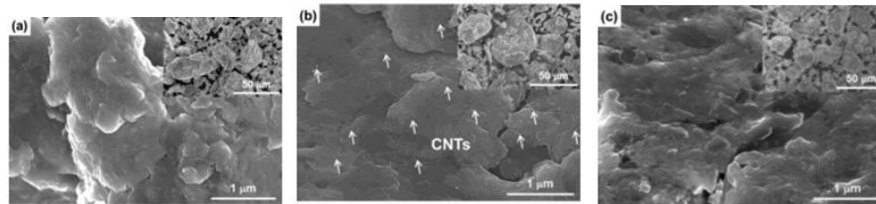


Fig. 2. SEM micrographs of as-milled (a) NiTi powder, (b) 0.5 vol% CNT/NiTi composite powder and (c) 1.0 vol% TiC/NiTi composite powder with insets of low magnification micrographs.

Fig. 3 shows the microstructure and the EDS spectra of the NiTi, and the 0.5 vol% CNT/NiTi and 1.0 vol% TiC/NiTi composites. EDS was used to determine the elemental composition of the different regions in the sample. The SEM micrographs in Fig. 3 show a dark phase (black circle) that corresponds to the NiTi matrix phase, and a lighter phase (red circle) that corresponds to Ti₂Ni, which exists mainly at the grain boundary^[2].

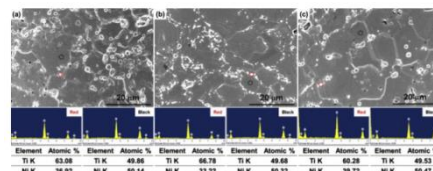


Fig. 3. Microstructural and EDS elemental analyses of the various regions of the (a) NiTi, and the (b) 0.5 vol% CNT/NiTi and (c) 1.0 vol% TiC/NiTi composites.

Red circles for lighter phase and black circles for dark phase. (For interpretation of the references to colour in this figure legend, the reader is referred to the web version of this article.) XRD patterns of the NiTi, and the 0.5 vol% CNT/NiTi and 1.0 vol% TiC/NiTi composites are shown in Fig. 4.

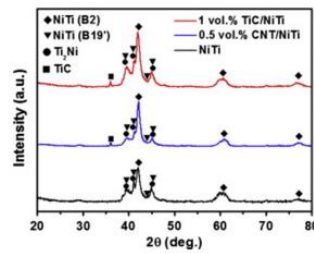


Fig. 4. XRD patterns of the NiTi, the CNT/NiTi and TiC/NiTi composites.

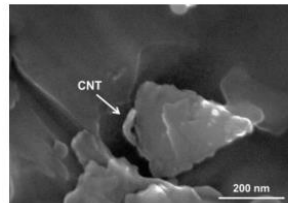
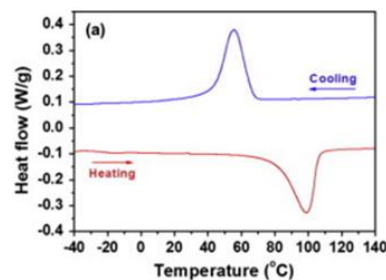


Fig. 5. SEM micrograph showing unreacted CNT on etched surface of the 0.5 vol% CNT/NiTi composite.

The formation of TiC by the reaction of CNTs or carbon black with Ti has been reported in previous studies [3-5]. However, some CNTs remained unreacted, with a cylindrical morphology and an approximate 20-nm diameter, and can be seen on the etched surface of the 0.5 vol% CNT/NiTi composite in Fig. 5.

Fig. 6 shows DSC curves of the NiTi, the 0.5 vol% CNT/NiTi and 1.0 vol% TiC/NiTi composites. Phase transformations occurred in the NiTi and in the composites during both cooling and heating, which demonstrates that all of the samples had shape memory. In Fig. 6, only one phase transformation peak could be observed in all of the DSC curves of the samples during cooling and heating, corresponding to $B2 \rightarrow B19'$ and $B19' \rightarrow B2$, respectively. The phase transformation temperatures and thermal hysteresis of the NiTi and the composites are listed in Table 2. Note that thermal hysteresis is defined as the difference between the austenitic finish temperature (A_f) and the martensitic start temperature (M_s)^[6]. With the addition of CNTs into the NiTi, the phase transformation temperatures decreased due to the reaction between the CNTs and Ti. This result agrees with those of previous studies^[6-8], which have shown that phase transformation temperatures decrease as the Ni/Ti ratio increases. Thermal hysteresis in the 0.5 vol% CNT/NiTi composite was greater than that in the NiTi. Likewise, the addition of 1.0 vol% TiC to the NiTi matrix increased the thermal hysteresis. It is generally thought that the addition of hard reinforcements to a NiTi matrix enlarges thermal hysteresis due to increased frictional resistance to interfacial motion between $B19'$ and $B2$ in the NiTi matrix. In addition, lattice mismatch between the reinforcements and the NiTi matrix relaxes the elastic strain energy, which is the driving force for the reverse phase transformation ($B19' \rightarrow B2$)^[9]. Thus, the thermal hysteresis measurements indicated that the phase transformation of the 0.5 vol% CNT/NiTi composite was less affected by the CNT reinforcements than that of the 1.0 vol% TiC/NiTi composite.



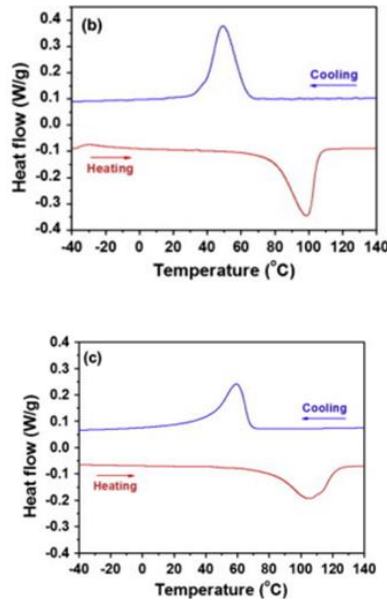


Fig. 6. DSC curves of the (a) NiTi, (b) 0.5 vol% CNT/NiTi and (c) 1.0 vol% TiC/NiTi composites. Shape recovery tests were performed by sequentially loading and unloading the NiTi, and the 0.5 vol% CNT/NiTi and 1.0 vol% TiC/NiTi composites during tensile tests under M_f , followed by heating to above A_f . The results of these shape memory tests are presented in Fig. 7. When 0.5 vol% CNT was added to the NiTi matrix, the shape memory effect was less degraded than when 1.0 vol% TiC was added. This shows that the 0.5 vol% CNT had a weaker effect on reverse phase transformations from B19' to B2 than did the 1.0 vol% TiC. This is in agreement with the wider interval between the reverse transformation temperatures (A_f - A_s) of 1.0 vol% TiC/NiTi composite than that of 0.5 vol% CNT/NiTi composite as shown in Fig. 6

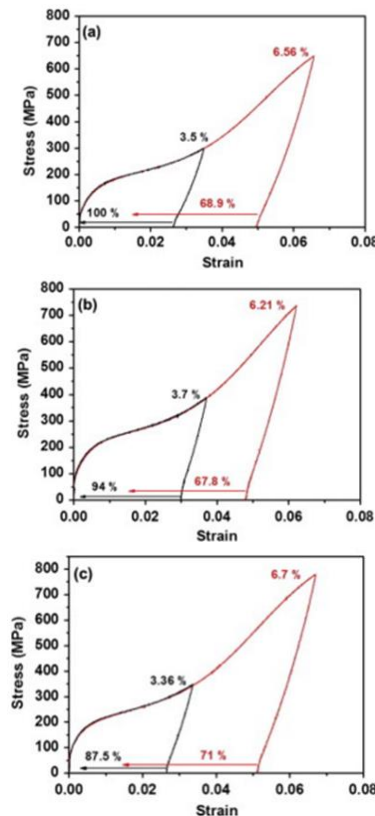


Fig. 7. Shape memory tests performed by sequential loading and unloading of the (a) NiTi, (b) 0.5 vol% CNT/NiTi and (c) 1.0 vol% TiC/NiTi composites.

Fig. 8 shows stress–strain curves of the NiTi, and the 0.5 vol% CNT/NiTi and 1.0 vol% TiC/NiTi composites under Mf. All of the samples showed typical stress–strain curves of a shape memory alloy, with double yield points on the curve^[10]. Typical stress–strain curves of shape memory alloys can be separated into four regions^[11]. The martensite twins begin to reorient and is detwinned at the first yield point followed by elastic region of martensite of NiTi. This reorientation continues in the first plateau. Subsequently, fully detwinned martensite is deformed elastically up to the second yield point, with plastic deformation occurring in the second plateau. The yield strength, elastic modulus, and ultimate tensile strength of the NiTi, and the 0.5 vol% CNT/NiTi and 1.0 vol% TiC/NiTi composites, as determined from the stress–strain curves, are summarized in Table 3. The yield strength of the 0.5 vol% CNT/NiTi and the 1.0 vol% TiC/NiTi composites increased by 29% and 26%, respectively, relative to that of the NiTi. The CNTs and TiC present in the NiTi matrix constrained the reorientation of martensite twins, and thus enhanced the yield strength. The addition of CNTs also raised the tensile strength by 11%. The tensile strength of the 1.0 vol% TiC/NiTi composite was slightly higher than that of the NiTi. Note that small additions of CNTs to the NiTi matrix resulted in a greater enhancement in the mechanical properties, including improved strength and minimally reduced elongation, than did the addition of TiC. This was due to the presence of unreacted CNTs in the NiTi matrix, as seen in the fracture surface of the CNT/NiTi composite in Fig. 9. Also, slope of second elastic region of the 0.5 vol% CNT/NiTi composite is larger than that of NiTi in Fig. 8, which shows that effective load transfer from the NiTi matrix to the reinforcements occurs. This demonstrates that CNTs may be used as a reinforcement material with minimal impact on the intrinsic properties of a NiTi matrix.

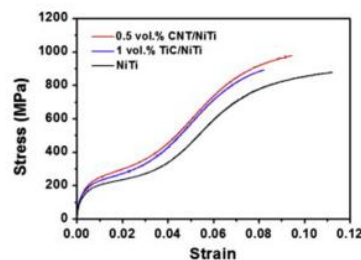


Fig. 8. Stress–strain curves of the NiTi, CNT/NiTi and TiC/NiTi composites.

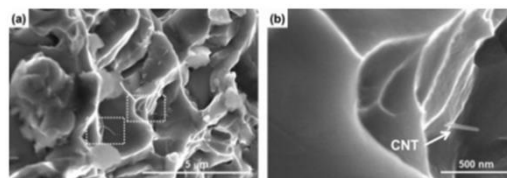


Fig. 9. CNTs observed at the fracture surface of the 0.5 vol% CNT/NiTi composite; (a) low magnification and (b) high magnification.

4. Conclusions

CNT/NiTi composites mixed with 0.5 vol% CNTs were prepared by high-energy ball milling followed by a powder metallurgical process in an effort to improve the mechanical strength of NiTi. For comparison, an NiTi alloy and a TiC/NiTi composite containing 1.0 vol% TiC were also prepared using the same fabrication process. The shape memory behavior of the 0.5 vol% CNT/NiTi composite was only slightly degraded relative to the NiTi while the shape memory effects was further degraded in the 1.0 vol% TiC/NiTi composite relative to the 0.5 vol% CNT/NiTi composite. The elastic modulus, yield strength and ultimate tensile strength of the 0.5 vol% CNT/NiTi composite was greater than that of the NiTi or the 1.0 vol% TiC/NiTi composite. Relatively small additions of CNTs had little influence on the shape memory effects of the NiTi while improving the mechanical strength due to the presence of unreacted CNTs in the NiTi matrix.

Acknowledgements

This work is supported by the National Natural Science Foundation of China (No. 11602066) and the National Science Foundation of Heilongjiang Province of China (QC2015058 and 42400621-1-15047), the Fundamental Research Funds for the Central Universities.

References

- [1] K. Otsuka, X. Ren. “Physical metallurgy of Ti–Ni-based shape memory alloys”[J]. *Progress in Materials Science*, 2005, 50(5):511-678.
- [2] Li B Y, Rong L J, Li Y Y. “Porous NiTi alloy prepared from elemental powder sintering”[J]. *Journal of Materials Research*, 1998, 13(10):2847-2851.
- [3] Feng X, Sui J H, Cai W, et al. “Improving wear resistance of TiNi matrix composites reinforced by carbon nanotubes and in situ TiC”[J]. *Scripta Materialia*, 2011, 64(9):824-827.
- [4] Threrujirapapong T, Kondoh K, Imai H, et al. “Mechanical Properties of a Titanium Matrix Composite Reinforced with Low Cost Carbon Black via Powder Metallurgy Processing”[J]. *Materials Transactions*, 2009, 50(12):2757-2762.
- [5] Ci L, Ryu Z, Jin-Phillipp N Y, et al. “Investigation of the interfacial reaction between multi-walled carbon nanotubes and aluminum”[J]. *Acta Materialia*, 2006, 54(20):5367–5375.
- [6] Frenzel J, Zhang Z, Somsen C, et al. “Influence of carbon on martensitic phase transformations in NiTi shape memory alloys”[J]. *Acta Materialia*, 2010, 55(4):1331-1341.
- [7] Yin Y, Kakeshita T, Choi M S, et al. “Martensitic transformation and anomalies in resistivity of (Ti–50Ni)_{1-x}C_x (x=0.1, 0.5at.%) shape memory alloys”[J]. *Journal of Alloys & Compounds*, 2008, 464(1–2):422-428.
- [8] Hamilton R F, Sehitoglu H, Chumlyakov Y, et al. “Stress dependence of the hysteresis in single crystal NiTi alloys”[J]. *Acta Materialia*, 2004, 52(11):3383-3402.
- [9] Melton K N, Mercier O. “The mechanical properties of NiTi-based shape memory alloys”[J]. *Acta Metallurgica*, 1981, 29(2):393–398.
- [10] K.N. Melton, O. Mercier “The mechanical-properties of NiTi-based shape memory alloys *Acta Metall.*” 29 (1981), pp. 393–398
- [11] Liu Y, Xie Z, Humbeeck J V, et al. “Asymmetry of stress–strain curves under tension and compression for NiTi shape memory alloys”[J]. *Acta Materialia*, 1998, 46(12):4325–4338.